Submitted to Journal of
Chemical Physics

UCRL-20314
Preprint

c.2

RECEIVED
LAWRENCE
RADIATION LABORATORY

NOV 17 1970

LIBRARY AND
DOCUMENTS SECTION

DETECTION OF IODINE ATOMS BY AN ATOMIC FLUORESCENCE TECHNIQUE: APPLICATION TO STUDY OF DIFFUSION AND WALL RECOMBINATION

Leo Brewer and Joel B. Tellinghuisen

September 1970

AEC Contract No. W-7405-eng-48

TWO-WEEK LOAN COPY

This is a Library Circulating Copy which may be borrowed for two weeks. For a personal retention copy, call Tech. Info. Division, Ext. 5545

UCRL-20314 c.2

LAWRENCE RADIATION LABORATORY
UNIVERSITY of CALIFORNIA BERKELEY

DISCLAIMER

This document was prepared as an account of work sponsored by the United States Government. While this document is believed to contain correct information, neither the United States Government nor any agency thereof, nor the Regents of the University of California, nor any of their employees, makes any warranty, express or implied, or assumes any legal responsibility for the accuracy, completeness, or usefulness of any information, apparatus, product, or process disclosed, or represents that its use would not infringe privately owned rights. Reference herein to any specific commercial product, process, or service by its trade name, trademark, manufacturer, or otherwise, does not necessarily constitute or imply its endorsement, recommendation, or favoring by the United States Government or any agency thereof, or the Regents of the University of California. The views and opinions of authors expressed herein do not necessarily state or reflect those of the United States Government or any agency thereof or the Regents of the University of California.

Detection of Iodine Atoms by an Atomic Fluorescence Technique: Application to Study of Diffusion and Wall Recombination.

Leo Brewer and Joel B. Tellinghuisen*

Inorganic Materials Research Division,
Lawrence Radiation Laboratory,
and Department of Chemistry, University of California,
Berkeley, California 94720

Abstract

An atomic fluorescence method has been used to detect iodine atoms in concentrations lower than $10^{10}/cm^3$. The heart of the apparatus is a "solar-blind" photomultiplier having practically no sensitivity to radiation of wavelengths longer than 2500 A, but with good response in the region of the two strong iodine atomic resonance lines near 1800 A. In combination with a small photolysis flashlamp, the system is used to study recombination of ground state ($^2P_{3/2}$) iodine atoms in pure I_2 vapor. At pressures below .2 torr the removal of atoms is seen to be predominantly a first-order diffusion-controlled process, characterized by a wall sticking probability of .047-.076 and a binary diffusion cross section of 100 A^2. The reaction $I(^2P_{3/2}) + I_2 \rightarrow I_3$ is found to be of minor significance in this study; a rough estimate indicates that fewer than one in 10^4 $I-I_2$ collisions lead to the formation of I_3.

* Present address: Department of Chemistry, University of Canterbury, Christchurch 1, New Zealand.

I. Introduction

The termolecular recombination of iodine atoms

$$I + I + M \xrightarrow{k_r} I_2 + M \qquad (1)$$

has been studied exhaustively in the years since 1936, when Rabinowitch and Wood first investigated the process.[1] In the 1950's this reaction was the basis of the prototype experiment of the several groups that were developing and refining techniques of flash photolysis.[2] When the problems involving thermal effects of the intense flashes were sorted out, the various workers obtained essentially consistent results for k_r for most foreign gases M. The notable exception was $M = I_2$, where estimates for k_r still range over a factor of four.[3]

Iodine atom recombination has also received plenty of theoretical attention, most such work being directed toward evaluating the relative contributions of two proposed mechanisms for the reaction--the energy-transfer mechanism

$$I + I \underset{k_{-1}}{\overset{k_1}{\rightleftharpoons}} I_2^* \qquad (2a)$$

$$I_2^* + M \xrightarrow{k_2} I_2 + M$$

and the bound-complex mechanism

$$I + M \underset{k_{-1}}{\overset{k_1}{\rightleftharpoons}} IM \qquad (2b)$$
$$IM + I \xrightarrow{k_2} I_2 + M$$

Calculations indicate that the latter is the dominant process for all but the simplest third body M.[4] Since both I_2^* and most possible complexes IM must be extremely short-lived, the two mechanisms are experimentally practically indistinguishable. However, in the case of a stable complex IM, (2b) predicts that initially, while the IM concentration is building up to a steady-state level, the removal of iodine atoms will be first order in [I], even though the production of I_2 remains second order in [I]. (For appropriate values of k_1, k_{-1}, and k_2, most of the iodine atoms may be removed and tied up in the complex IM before appreciable formation of I_2 occurs.) The case M = I_2 is suspected to be of this type, as I_3 has been predicted to be stable by about 5 kcal/mole.[5] Unfortunately it has not been possible to detect I_3 either directly or indirectly in any of the existing kinetic studies.

One feature common to all the flash photolysis studies of I atom recombination has been the indirect determination of atom concentrations from changes in the I_2 visible absorption. To obtain good signal precision in the region of linear absorption by I_2, it is necessary to employ low I_2 concentrations and to photolyze a large fraction of the molecules present, which requires flashes of total energy 1000 joules or more; this in turn introduces the thermal complications mentioned above. Such problems are minimized by increasing the diluent gas pressures. With these procedures, however, it is impossible to observe the recombination of I atoms in pure I_2 vapor. Instead, values for k_{r,T_2} have been estimated from corrective terms to the composite

recombination in some foreign gas, usually argon. A method involving direct observation of iodine atoms would have obvious value here and in the study of other I atom reactions.

Existing methods of direct observation of ground state ($^2P_{\frac{3}{2}}$) iodine atoms include ESR techniques used by several workers to follow I atom concentrations under conditions of steady-state photolysis of I_2,[6,7,8] and a photographic atomic absorption method utilized by at least one group in a number of kinetic flash spectroscopic studies.[9] Recently we have used a simple but effective atomic fluorescence method to observe iodine atoms under both transient and steady-state conditions[10]. With a low-power microwave discharge lamp as source of atomic resonance radiation, and a commercially produced "solar-blind" photomultiplier to monitor resonance fluorescence at 1783 A, we have been able to detect iodine atoms in concentrations lower than $10^{10}/cm^3$. Employing a small (~15 joule) photolysis flash of duration ~25 μsec, we have used this method to investigate I atom recombination in pure I_2 vapor. The strong UV absorption by molecular iodine has restricted our observations to I_2 pressures lower than .2 torr, where diffusion-controlled wall recombination dominates the removal of atoms. However, we have been able to obtain a rough upper limit to the rate for the reaction

$$I(^2P_{3/2}) + I_2 \xrightarrow{k_{I_3}} I_3 \qquad (3)$$

as well as a measure of the binary I-I_2 diffusion coefficient and the sticking coefficient for I atoms on "clean" silica.

II. Detection of Resonance Fluorescence

The resonance lines of atomic iodine fall in the vacuum ultraviolet region of the spectrum. The two of longest wavelength occur at 1830 A and 1783 A and are the only resonance transitions of importance in this work. Lifetime measurements[11] and absorption data[10] indicate that the 1783 A 6s $^2P_{3/2} \leftrightarrow 5p^5\ ^2P_{3/2}$ transition, with an A value of 2.5×10^8/sec, is 15-20 times stronger than the spin-forbidden 1830 A 6s $^4P_{5/2} \leftrightarrow 5p^5\ ^2P_{3/2}$ transition. Other important lines in the $^2P \leftrightarrow {}^2P$ multiplet are the 2062-A and 1799-A lines, both of which connect with the $^2P_{\frac{1}{2}}$ metastable lower level. Natural iodine is 100% I^{127} with nuclear spin 5/2, so all the above "lines" actually consist of a number of hyperfine components--10,12, and 6, respectively, for the 1783, 1830, and 2062 lines, for example.

The dependence of fluorescence signal on concentration of absorbers has been discussed at length elsewhere[10], but a few points are worthy of emphasis here. Consider the situation depicted in Fig. 1, in which a cell is irradiated at one end, and fluorescence is observed at right angles some distance down the cell from the entrance window. In general the detector sees a signal consisting of scattered light and fluorescence, both of which depend on the efficiency of the detector, the geometry of the arrangement, and the concentration of the absorbing species. With a linear quantum detector such as a photomultiplier operated

in the current mode, the signal will be proportional to the total quantum flux, which, for fixed geometry and constant radiation distribution, will depend in a simple way on the concentration of absorbers N. We will assume that the quantum yield of fluorescence is independent of the concentration N (i.e. no self-quenching). Then for concentrations low enough that the mean free path of a photon at the resonance frequency is greater than the dimensions of the cell, the fluorescence signal will be directly proportional to the absorption occurring in the shaded region of Fig. 1. The scattered light signal in a cell of the type illustrated will be mostly due to scattering off the cell walls; it will have some maximum value at N = 0 and will decrease as N is increased. The total signal is given approximately by

$$\begin{aligned} \text{Signal} &= \text{const}_1 \int E_\nu e^{-k_\nu \ell}\left(1 - e^{-k_\nu b}\right) d\nu \\ &\quad + \text{const}_2 \int E_\nu e^{-k_\nu(\ell + a)}\, d\nu \end{aligned} \tag{3}$$

where E_ν is the frequency distribution of the exciting light, and k_ν is the absorption coefficient of the absorbing gas.

For this work both E_ν and k_ν are effectively determined by Doppler broadening and may be adequately represented

$$\begin{aligned} E_\nu &= C e^{-\beta' \omega^2} \\ k_\nu &= k_0 e^{-\beta \omega^2} \end{aligned} \tag{4}$$

where $\omega = \nu - \nu_0$ and $\beta = 4 \ln 2/(\Delta\nu_D)^2$. Here ν_0 is the resonance frequency, $\Delta\nu_D$ is the Doppler width (full width at half peak height), and k_0 is proportional to the concentration N. From the

first term in Eq. (3) we see that the fluorescence signal first rises linearly with N, eventually attains a maximum, and then decreases with any further increase in N, as the exciting radiation reaching the shaded region is progressively attenuated. The behavior of Eq. (3) is displayed quantitatively in Fig. 2. The value of the ratio $const_1/const_2$ was chosen to represent the conditions actually encountered in these experiments, where the maximum fluorescence signal was about five times the maximum scattered-light signal. γ is a relative linewidth parameter, $\gamma = \beta/\beta'$; s is the relative line strength, so that k_o is proportional to s x N. Concentrations are in arbitrary units, but it is useful to know that the maximum signal falls at $(k_o \ell) = 1.12$ when $\gamma = 1$ and $b/\ell = 0.2$. (Without the scattered-light term the maximum shifts to $(k_o \ell) = 1.22$.)

The fluorescence function curves in Fig. 2 cannot be applied quantitatively to the present situation for several reasons. First, when the concentration is such that $(k_o \ell) > 1$, radiation diffusion begins to play a role in determining the fluorescence signal[12]. Second, the existence of hyperfine structure in the resonance lines complicates the situation somewhat. The net effect is to weaken the apparent absorption, so that for I atoms absorbing at 1783 A the fluorescence maximum occurs at a concentration about six times greater than the value calculated assuming a single Doppler-broadened line[13]. Finally, molecular iodine strongly absorbs the atomic resonance radiation, decreasing and modifying the exciting lines

in an unknown manner and contributing a molecular fluorescence signal to the total background.

Even though the fluorescence curves in Fig. 2 cannot be applied rigorously to the present situation, they provide some useful information. From atomic absorption data[10] the signal maximum (for a cell with $\ell = 40$ mm) occurs at a concentration of about 10^{12} iodine atoms per cm^3, in the absence of the complicating effects of the I_2 UV absorption. If measurements are restricted to signals less than 20% of the maximum, where concentrations are less than $10^{11}/cm^3$, the dependence of signal on concentration is practically linear; and the treatment of data is accordingly simplified. For I_2 pressures lower than ~300 mtorr (the vapor pressure at room temperature), the molecular UV absorption is no insurmountable problem. Thus atomic fluorescence should provide a simple and quite sensitive method for observing ground state I atoms in kinetic situations.

III. Kinetics of Iodine Atom Removal

A. General

From the work of Rabinowitch and Wood[1] we know that at foreign gas pressures lower than 50 torr, wall recombination governs the removal of iodine atoms, and the rate is diffusion-limited. In pure I_2 vapor homogeneous recombination may prevail at pressures much lower than this because of the great efficiency of the I_2 molecule as a third body. However, we might reasonably

expect wall recombination to predominate at I_2 pressures lower than ~0.5 torr, though the overall rate may include an appreciable contribution from homogeneous processes.

In the limit of low I_2 concentrations the I atom mean free path exceeds the dimensions of the cell, and the removal rate should approach a constant value determined solely by the nature of the surfaces and the cell geometry. One possible mechanism may be summarized

$$I \underset{k_{-1}}{\overset{k_1}{\rightleftharpoons}} I_{wall} \tag{5a}$$

$$I + I_{wall} \xrightarrow{k_2} I_{2,wall} \tag{5b}$$

$$I_{2,wall} \underset{k_{-3}}{\overset{k_3}{\rightleftharpoons}} I_2 \tag{5c}$$

If the vapor phase-adsorbed I_2 equilibration is very rapid, or if a transient buildup of adsorbed I_2 does not affect the I atom removal processes, we may neglect (5c) in the detailed mechanism[14]. Then if we further assume that the surface concentrations are in equilibrium with the gas phase concentrations at all times, we may use the adsorption isotherm approach to obtain

$$-\frac{d[I]}{dt} = 2\,k_2\,[I]\left\{\frac{k_1\,[I]}{k_{-1} + (k_1 + k_2)[I]}\right\} \tag{6}$$

where the term in braces is θ, the fraction of available sites that are occupied.

Equation (6) predicts that the reaction will be second order in [I] for low surface coverage and first order in the limit

of high occupancy. Unfortunately the situation is far more complex. A study by Campbell and co-workers[15] indicated that at room temperature I_2 is strongly adsorbed on glass at quite low pressures, and furthermore that the process follows the Langmuir dissociative adsorption isotherm. From their results half-monolayer coverage of iodine atoms is achieved at an I_2 pressure of ~14 mtorr. At 1 mtorr, the coverage is still roughly 20%. The present study involved pressures greater than 4 mtorr, so in view of the relatively small number of iodine atoms (~10^{13}) produced by the flash, we can assume that the value of θ is effectively fixed by the I_2 adsorption equilibrium

$$I_2 \rightleftharpoons 2\, I_{wall} \tag{7}$$

$$\theta = \frac{a\,[I_2]^{1/2}}{1 + a\,[I_2]^{1/2}} \tag{8}$$

Then it is conceivable that the only additional process of interest will be (5a), and the I atom removal will be strictly first order in [I].

As we increase the I_2 pressure the I atom decay rate should decrease, as the atoms must diffuse through the I_2 vapor to reach the walls. Therefore, until the homogeneous recombination sets in, the rate should go as $(1 + c\,[I_2])^{-1}$, giving

$$-\frac{d[I]}{dt} = \frac{k_w\,[I]}{1 + c\,[I_2]} \tag{9}$$

where k_w may vary with the I_2 pressure as the nature of the wall surface changes, and c is a parameter which depends in some way on the cross section for I-I_2 collisions.

B. Diffusion Kinetics

When the iodine atom mean free path is much smaller than the pertinent cell dimensions, the decay of the atom concentration will conform to the diffusion equation

$$\frac{\partial N}{\partial t} = D \nabla^2 N - \Gamma' N \tag{10}$$

where D is the diffusion constant, and the term $\Gamma' N$ is included to account for possible volume removal via a first-order I_3 bound-complex mechanism. Solutions to (10) for various cell configurations and boundary conditions have been discussed by Wise and co-workers[16], Crank[17], and Carslaw and Jaeger[18]. In the present study a cylindrical cell is employed, and the solutions take the form

$$N(r,t) = e^{-\Gamma' t} \sum_{n=1}^{\infty} A_n J_0\left(\frac{\alpha_n r}{r_0}\right) e^{-D\left(\frac{\alpha_n}{r_0}\right)^2 t} \tag{11}$$

J_0 represents the Bessel function of order zero, r_0 is the cell radius, and the A_n and α_n are chosen to satisfy the boundary conditions

$$N(r,t) = N_0 \quad \text{at} \quad t = 0 \tag{12a}$$

$$\int_{\text{surface}} \vec{\text{flux}} \cdot d\vec{S} = -\int_{\text{volume}} \frac{dN}{dt}\, dV \tag{12b}$$

The net outward flux per unit area at the cylinder wall is given by[19]

$$\text{flux} = \epsilon\left[\frac{1}{4} N(r_0)\bar{v} - \frac{1}{2} D\left(\frac{\partial N}{\partial r}\right)_{r_0}\right] \tag{13}$$

where ϵ is the sticking probability per wall collision, and

$\bar{v}$ is the mean iodine atom speed. Thus (12b) appears in the form

$$\alpha_n J_1(\alpha_n) = \left(\frac{\epsilon}{2-\epsilon}\right) \frac{h_n \bar{v}}{2D} J_0(\alpha_n) \tag{14}$$
$$= h' J_0(\alpha_n)$$

and the constants A_n become[20]

$$A_n = \left(\frac{2h'}{\alpha_n^2 + h'^2}\right) \frac{N_0}{J_0(\alpha_n)} \tag{15}$$

From Equation (11) the overall decay will be a sum of exponentials. In general the terms for $n > 1$ are small and decay rapidly leaving essentially a single exponential function. Furthermore, if the detector samples the entire cross section of the cell evenly, the signal will be proportional to $\int_0^{r_0} N(r,t) r\, dr$, giving

$$\text{Signal} \propto e^{-\Gamma' t} \sum \frac{(h' r_0)^2}{\alpha_n^2(\alpha_n^2 + h'^2)} e^{-D\left(\frac{\alpha_n}{r_0}\right)^2 t} \tag{16}$$

and the higher terms become even less significant than indicated by Eq. (15).

In the low-pressure limit the approximate rate $\Gamma \left(= \frac{\alpha_1^2 D}{r_0^2} + \Gamma'\right)$ approaches a constant value

$$\Gamma_0 = \frac{\bar{v}}{r_0}\left(\frac{\epsilon}{2-\epsilon}\right) \tag{17}$$

For intermediate I_2 concentrations, the pressure dependence of Γ is complex, but at high pressures α_1 approaches a constant value, so that $(\Gamma - \Gamma')$ displays an inverse dependence on $[I_2]$. Calculations show that the overall pressure dependence of $(\Gamma - \Gamma')$ in the region of interest here is quite adequately described by the

form suggested in Eq. (9), though the relationship between the diffusion coefficient and the constant c in Eq. (9) is not straightforward. However, for the range of h' values encountered in this study, c is given approximately by the expression

$$c[I_2] = .17\ k_w r_0^2/D \qquad (18)$$

where k_w is equivalent to Γ_0 in Eq. (17)[21].

IV. Experimental

The equipment utilized in this study has been described in detail elsewhere[10], but a brief review is in order here. The basic setup was the quintessence of simplicity: It consisted of a solar-blind photomultiplier and power supply, a fused silica reaction cell having three Suprasil windows with a discharge lamp affixed directly to the cell, a microwave power supply to run the lamp, a small flashtube operated off a simple capacitor circuit, and an oscilloscope with camera for recording the signals.

The photomultiplier was an EMR[22] Model 541H-08-18, labeled "extreme solar blind" by the manufacturer. This tube is of the end-on type with the housing designed to accommodate an "O"-ring, which provides a very effective vacuum seal. The photocathode material is CuI, for which spectral response curves have been given by Dunkelman[23]. In addition the relative sensitivity for this particular instrument was determined in this lab by observing its response to six iodine atomic lines from a source previously calibrated with sodium salicylate and an RCA 1P21

multiplier. Results showed that the efficiency drops off rapidly from 1800 A to 2100 A, with the sensitivity at 2062 A less than 1/100 that at 1783 A. The tube is for all practical purposes totally blind to all radiation in the visible.

The fused silica photolysis cell was about 110 mm long with an inside diameter of 36 mm. The iodine discharge lamp was attached directly to one end of the cell; evacuatable observation ports were situated at the other end and on the side about 40 mm from the lamp, for detection of absorption and fluorescence, respectively. The evacuatable ports allowed us to fasten the photomultiplier rigidly against the cell and at the same time avoid absorption by air[24]. A "cold-finger" was appended to the cell near the rear window to provide for convenient control of the I_2 pressure. Before use the cell was flamed out under vacuum ($\sim 10^{-5}$ torr), charged with distilled, resublimed iodine, and sealed off with a torch.

The iodine lamp was charged with excess iodine and enough spectroscopic-grade argon ($\sim$1 torr) to maintain a stable, homogeneous discharge when the I_2 was frozen out in the lamp cold-finger at the temperature of liquid nitrogen. The lamp was flamed with a torch and flushed with Ar several times until examination with a hand spectroscope revealed no prominent molecular impurities in the visible output. Then it was sealed off and the lamp-cell was removed for collection of data. In use the lamp was powered by a 100-watt hospital-type microwave generator fitted

with a Type A directional antenna. Optimum fluorescence signal-to-noise conditions were obtained with the lamp cold-finger maintained at -80° in an ethanol-dry ice bath, but coolant temperatures as high as -40° and as low as -196° proved practicable as well.

A xenon-filled flashtube, Model FP-5, manufactured by Xenon Corporation, was used to photolyze the I_2. Although this tube is recommended for use at voltages as high as 10 kV and energies of 500 joules, such violent flashes were unnecessary and undesirable in this work. Hence the flashtube was operated from a simple high hold-off circuit with external triggering provided by a microswitched Tesla coil[25]. With a charging capacitance of 4 μf and a potential of 2800 volts, the energy per flash was only 15 joules. Under these conditions the flashes were generally repeatable to better than 3% in maximum intensity. The time dependence of the flash was investigated by displaying the signal from an RCA 935 phototube on the screen of a Tektronix 585 oscilloscope. The rise time was 5 μsec, and the 1/3-peak-height time was 12 μsec. 90% of the total energy was dissipated in the first 12 μsec, with less than 2% of the emission coming after 25 μsec.

In operation the flashtube was placed in a box $\frac{1}{2}$ meter from the photolysis cell, with its axis parallel to that of the cell. The light emerged from a 7 cm x 7 cm hole, where the unwanted UV component was eliminated with a Kodak Wratten No. 16 filter. (In some experiments the exciting flash was further weakened

with Wratten neutral density filters.) The I atom fluorescence signal was developed across a 240 KΩ resistor and observed and photographed on the screen of the oscilloscope operated in the single-trace mode. The horizontal sweep could be triggered by the signal itself. To avoid distortion, tracings were recorded using the DC input mode, with a Type W plug-in unit to null the background so that the transient signal could be observed full scale on the screen. Peak signals were accordingly 1-4 volts. The tracings were photographed on Polaroid 3000 roll film, and base lines were always recorded immediately after the flash tracings to minimize the effects of slow drifts in the iodine lamp output.

The RC time constant of the recording circuitry was reduced by using short lengths of coaxial cable. Direct observation of the UV component of the flash through the detection circuitry yielded a decay time of 40-50 μsec, a value four times greater than the true time, but still less than 1/20 of the mean exponential decay time for the fastest recorded I atom recombination tracing.

Iodine atom decay curves were photographed for I_2 pressures from 4 to 160 mtorr, corresponding to cold-finger temperatures from -18 C to 18 C. The curves were later analyzed with the aid of an opaque projector. I_2 vapor pressures were calculated from the free energy functions given by Shirley and Giauque[26] for solid I_2 and the JANAF Tables[27] for I_2 vapor and for the enthalpy of sublimation of I_2.

V. Results and Discussion

Some typical tracings are illustrated in Fig. 3. Whereas photos (a-c) seem to be well-behaved decay curves, photo (d) exhibits distortion due to effects of nonlinearity in the fluorescence function. To lessen complications of this sort it was necessary to attenuate the flash with neutral density filters until the maximum working signal was less than ~25% of the greatest achievable signal. Further attenuation demonstrated that any systematic error at this level was well within the precision of the data[28]. Plots of log(Signal) versus time for I_2 pressures greater than ~30 mtorr were clearly linear, although curves recorded at pressures below ~25 mtorr seemed to display slight deviation from first-order decay. Figure 4 shows the semi-log plots for (a) and (b) in Fig. 3. The deviation from linearity is quite pronounced in Fig. 4a. Such behavior seems to indicate that some second-order I-atom removal is occurring at these low pressures. This interpretation contradicts the expectations set forth in Section III-A; a possible explanation will be presented shortly.

The forty-odd data points from each tracing were treated in terms of a weighted linear logarithmic fit. Results are displayed in Fig. 5, where the exponential time constant Γ^{-1} is plotted against P_{I_2}. The behavior predicted by the diffusion treatment and approximately by Eq. (9) (with k_w a constant) is borne out only roughly by these results. Instead there appears to be a short plateau at low P_{I_2} and a slight falloff in Γ^{-1} at the higher I_2 concentrations. The plateau may be partly a mathematical

irregularity arising from the deviation from first-order kinetics at low I_2 pressures. In any case the anomalous behavior in this region can probably be attributed to the changing nature of the silica surface, as dictated by the dissociative adsorption (7) and by nondissociative physisorption of I_2, which must set in at pressures greater than ~10 mtorr. Physisorption isotherms typically level off at $P/P_0 \approx .1$. For I_2 at room temperature P_0 is about 300 mtorr, so "monolayer" coverage should be complete around 30 mtorr; and the isotherm should rise only slightly thereafter in the range covered by Fig. 5. In that case the leveling-off tendency in the points for I_2 pressures greater than 100 mtorr may indicate the onset of homogeneous recombination. On this assumption we can estimate the rate of formation of I_3.

In terms of the diffusion treatment the existence of the low-pressure plateau in Γ^{-1} implies that the sticking probability ϵ is increasing in the range 5-30 mtorr, effectively counterbalancing the diffusion-hindered transport of I atoms to the wall. The apparent zero-pressure intercept is 3.4 msec, which from Eq. (17) gives $\varepsilon = 0.047$ for the sticking probability per wall collision[29]. If we further accept that ε increases until $P_{I_2} \approx 30$ mtorr, then remains essentially constant, the rise in Γ^{-1} in the range 30-80 mtorr is entirely ascribable to diffusion retardation. When the points in this region are fit to Eqs. (11) and (14), the best values of ε and the diffusion coefficient are found to be 0.076 and 7.8 torr cm^2/sec, respectively.[30] (These values have been used to produce the curve in Fig. 5.)

From Fig. 5 we can estimate that Γ' is ~20/sec at 150 mtorr I_2, implying that only one in ~10^4 I-I_2 collisions leads to the formation of I_3, if this interpretation is valid. If the increase in the measured rate at these I_2 pressures is due to another rise in the wall sticking probability, the volume removal rate will be even lower, so the value $k_{I_3} = 4 \times 10^{-15}$ cm^3/sec represents a crude upper limit on the rate constant for this process. This rate, though small, is still several orders of magnitude greater than the estimated three-body removal rate for I atoms in the concentrations encountered here[31].

In deriving the value 7.8 for the diffusion constant we treated the cell as an infinite cylinder and used the appropriate equations from Section III. When consideration is given to the finite length of the cell[20], it is found that measured decay rates will be 5-15% higher than for the assumed infinite cylinder. However, in light of the extensive interpretation of Fig. 5 required to arrive at the above number, we feel that the value D(STP) = 0.009 (±25%) cm^2/sec adequately and accurately reflects this study's measure of the $I(^2P_{3/2})$-I_2 binary diffusion constant. The value for D may be related to a cross section for diffusion by means of the rigorous expression for a hard-sphere model[32],

$$D_{12} = \frac{3}{32 N d^2} \left(\frac{8 kT}{\pi \mu} \right)^{1/2} \qquad (19)$$

where μ is the reduced mass for the collision partners and d^2 is the cross section. From (19) d^2 is 100 A^2, which is more than six times the gas-kinetic cross section.

The deviation from first-order kinetics for I_2 pressures lower than ~25 mtorr is somewhat puzzling. Eq. (6) predicts second-order atom removal in the limit of low surface coverage. However, the value of θ should be practically independent of flash-produced atoms, because the latter, according to Eq. (8), are inconsequential in comparison with the number of occupied sites for even the lowest I_2 pressure involved. In that case mechanism (5) cannot be invoked. On the other hand Campbell and colleagues[15] found that the I_2 adsorption is quite sensitive to changes in the nature of the glass surface, so it is possible that Eqs. (7) and (8) do not apply in the present situation. It might be noted that in a steady-state photolysis experiment, Wassermann and co-workers[8,33] found the wall removal of I atoms to be strictly second order in acid-treated silica cells, whereas under similar conditions we found only nominal deviation from first-order kinetics.[10] Clearly the problem is too complex to be resolved in this work. However it might be suggested that in addition to processes (5a,b) there exists the bimolecular wall removal

$$2\ I \xrightarrow{k_w'} I_{wall} \cdot I_{wall} \qquad (20)$$

requiring adjacent surface sites. The constants k_w and k_w' are of course strongly dependent upon specific surface conditions; but relatively speaking, second-order removal will be favored for low surface coverages and first-order for high. Such a

competitive second-order process is consistent with the observed dependence of ϵ on P_{I_2}. The increase in ϵ with P_{I_2} shows clearly that I atoms stick preferentially adjacent to or on other adsorbed atoms and/or molecules (i.e. that (5b) is the dominant process for removal of transient atoms).

The value of 100 A^2 for the $I-I_2$ diffusion cross section is surprisingly large. By comparison, values for several other atom-parent molecule pairs are much nearer the analogous gas-kinetic cross sections: 5.0 A^2 for $H-H_2$ [34], 9.6 A^2 for $O-O_2$ [35], and 9.9 A^2 for $N-N_2$ [36], for example. The extraordinarily large value for $I-I_2$ lends support to the idea of a short-lived I_3 rotational complex, suggested by Hershbach and co-workers[37]. On the other hand the low upper boundary on the rate constant for $I + I_2 \rightarrow I_3$ indicates that the strong $I-I_2$ interactions are still not sufficient to produce appreciable concentrations of I_3 for the low I_2 pressures involved here.

The sticking efficiency of 0.047-0.076 for I atoms on silica is also quite high in comparison with values for other atoms. There seems to be a wide disparity in reported ϵ values, probably reflecting the sensitive dependence on surface conditions. Typical values for O and N atoms are around 10^{-3}-10^{-4}.[35] Ogryzlo[38] has reported measurements for halogen atoms on acid-coated surfaces. He found values of 4-6 x 10^{-5} for Cl and Br atoms but was unable to obtain results for I atoms, because the latter appeared to recombine rapidly in the hot, uncoated section of his apparatus. However, other studies [10,33] have demonstrated that

for I atoms on acid-coated surfaces the sticking efficiency drops to 10^{-2}–10^{-3}.

VI. Conclusions

Detection of atomic fluorescence is seen to provide an effective, sensitive technique for observing iodine atoms under transient conditions. Such a method has been used to study the heterogeneous recombination of I atoms in I_2 vapor, yielding approximate values for the binary diffusion coefficient and the sticking efficiency for I atoms striking "clean" silica surfaces. Homogeneous recombination via a stable I_3 complex is found to be relatively unimportant for I_2 pressures lower than 200 mtorr.

The flash-photolysis atomic-fluorescence technique used in this work should be widely applicable to studies of reactions of certain atoms. The advantage of simplicity is obvious; but more important is the extreme sensitivity of the detection method, which allows one to employ small perturbative flashes instead of cataclysmic ones. To our knowledge a method of this sort has been reported in the literature only once, that being the work by Braun and Lenzi[39], in which reactions of atomic hydrogen with olefins were followed by measuring absorption and fluorescence of Lyman-α radiation.

References

1. E. Rabinowitch and W. C. Wood, J. Chem. Phys. 4, 497 (1936).

2. R. G. W. Norrish and G. Porter, Nature 164, 658 (1949).

3. M. I. Christie, J. Am. Chem. Soc. 84, 4066 (1962).

4. H. S. Johnston, Gas Phase Reaction Rate Theory, (The Ronald Press Company, New York, 1966).

5. D. L. Bunker and N. Davidson, J. Am. Chem. Soc. 80, 5085 (1958).

6. K. D. Bowers, R. A. Kamper, and C. D. Lustig, Proc. Phys. Soc. B 70, 1176 (1957).

7. J. W. Mayo, (Ph.D. Thesis), Massachusetts Institute of Technology (June, 1964).

8. E. Wassermann, W. E. Falconer, and W. A. Yager, J. Chem. Phys. 49, 1971 (1968).

9. R. J. Donovan and D. Husain, Chem. Rev. 70, 489(1970).

10. J. B. Tellinghuisen, (Ph.D. Thesis), University of California, Berkeley; UCRL-19112 (November, 1969).

11. G. M. Lawrence, Astrophys. J. 148, 261 (1967).

12. If the upper level can decay to the ground state via only one path, as for the I 1830 resonance line, the effect would be

to shift the curves in Fig. 2 up slightly for $N > N_{max}$. If other paths are available the absorbed energy may exit in some manner not observable to the detector. Thus diffusion of 1783 radiation through atomic iodine will result in an increased yield of 2062 light at the detector, since these lines have the upper 6s $^2P_{3/2}$ level in common, and the population of the lower $^2P_{1/2}$ state should be nominal.

13. Calculations on the 1830 line, where the hyperfine structure has been worked out, indicate that the fluorescence function remains essentially constant in form when hyperfine structure is taken into account; that is, for given values of the fluorescence function, the corresponding concentrations for the two cases (complex lineshape vs. simple Gaussian parameters E_ν and k_ν) stand in constant ratio for the range of concentrations of interest here. For example, a resonance line with four equal, "separate" components would have a hyperfine correction factor of four, and the fluorescence functions for the two cases could be represented by the two curves for $\gamma = 3$ in Fig. 2. Unfortunately the hyperfine structure is not known experimentally for the strong 1783 line, but a value of six for the correction factor is quite reasonable. (See Ref. 10).

14. As it turns out, in this work each flash produced only enough I atoms to cover about one out of every 10^4 available surface sites.

15. J. S. Campbell, R. L. Moss, and C. Kemball, Trans. Faraday Soc. 56, 1481 (1960).

16. Y. Rajapakse and H. Wise, J. Chem. Phys. 48, 3361 (1968).

17. J. Crank, The Mathematics of Diffusion, (Oxford University Press, London, 1956).

18. H. S. Carslaw and J. C. Jaeger, Conduction of Heat in Solids, (Oxford University Press, London, 1947).

19. R. D. Present, Kinetic Theory of Gases, (McGraw-Hill Book Company, Inc., New York, 1958), p. 33.

20. The assumption of uniform initial concentration in Eq. (12a) may be a specious one in the present case, because of the arrangement of flash and cell. Any assymmetry will introduce into (11) terms in $\sin(n\theta)$, $\cos(n\theta)$ having Bessel functions of order one and greater. However, the initial degree of assymmetry should be small, and the error resulting from assuming (12a) is felt to be negligible.

Equation (11) is the solution for an infinite cylinder. For a finite cylinder Carslaw and Jaeger (p. 195) present the solution

$$N = \Psi(z, \ell, h)\, \chi(r, r_0, h)$$

where 2ℓ is the length of the cylinder and h is h'/r_0. The form of the radial part of the solution χ is still given by (11), with the same boundary equation (14). The axial part Ψ is given by

$$\Psi = \sum_{n=1}^{\infty} \frac{(2h)\cos(\beta_n z)\, e^{-D\beta_n^2 t}}{[(h^2+\beta_n)\ell + h]\cos(\beta_n \ell)}$$

subject to the boundary condition $\beta_n \tan(\beta_n \ell) = h$.

21. The theoretical curvature in a plot of Γ^{-1} vs. pressure is so slight over a range of h' values 0-20 as to be practically unobservable experimentally. The limiting slope at zero pressure gives 1/8 for the numerical coefficient in Eq. (18). However the slope in Γ^{-1} increases rapidly in the region $h' < 3$, and Γ^{-1} is practically linear thereafter with the value 0.17 for the coefficient.

22. Electro-Mechanical Research, Inc., Princeton, New Jersey.

23. L. Dunkelman, J. Quant. Spectrosc. Radiat. Transfer 2, 533 (1962).

24. Absorption of 1783 radiation by air is actually quite weak --about 15% for a 10-mm path length--so a mechanical pump was sufficient here.

25. It was later discovered that the flashtube could be fired by simply grounding the external triggering wire, as long as the voltage was ~2500 or more. This triggering mode was absolutely noise-free. It was, however, necessary to "recondition" the setup occasionally by firing with a Tesla coil.

26. D. A. Shirley and W. F. Giauque, J. Am. Chem. Soc. 81, 4778 (1959).

27. JANAF Thermochemical Tables, The Dow Chemical Company, Midland, Michigan, 1961.

28. Calculations indicate that the deviation from linearity in the fluorescence function is 10-15% at this level, which would produce an error of ~5% in the slope of the semi-log plot of a typical tracing. On the other hand, the higher-order decay terms in Eq. (11) contribute a deviation of roughly the same magnitude in the opposite direction. Because of the offsetting nature of these effects and the lack of high precision in the data, such problems were ignored.

29. This value may be slightly higher than the true zero-pressure limit, because from (8) the surface coverage is still ~35% at the lowest I_2 pressure investigated.

30. Because of the implicit relationship between ϵ, D, and the measured rates, the "best" values were determined by locating the minimum of the summed square deviations ($\sum(\delta y_i)^2$) in a matrix of pre-selected ϵ and D values.

31. Johnston (Ref. 4) quotes a value of 6.5×10^{-30} cm^6/sec for k_r, so the termolecular half-life of the atom concentration is more than 100 seconds under these conditions.

32. J. O. Hirshfelder, C. F. Curtiss, and R. B. Bird, Molecular Theory of Gases and Liquids, (John Wiley and Sons, Inc., New York, 1954).

33. E. Wassermann, W. E. Falconer, and W. A. Yager, Berichte der Bunsengessellschaft 72, 248 (1968).

34. B. Khouw, J. E. Morgan, and H. I. Schiff, J. Chem. Phys. 50, 66 (1969).

35. Robert S. Yolles and Henry Wise, J. Chem. Phys. 48, 5109 (1968).

36. J. E. Morgan and H. I. Schiff, Can. J. Chem. 42, 2300 (1964).

37. Y. T. Lee, J. D. McDonald, P. R. LeBreton, and D. R. Hershbach, J. Chem. Phys. 49, 2447 (1968). In a molecular-beam study this group found that the $Cl-Br_2$ complex breaks up in a time much shorter than a rotational period, but that the $Br-I_2$ complex survives about one rotational lifetime or 5×10^{-12} sec. Prof. Hershbach has since suggested that the $I-I_2$ complex might survive for ten or more rotational periods.

38. E. A. Ogryzlo, Can. J. Chem. 39, 2556 (1961).

39. W. Braun and M. Lenzi, Disc. Faraday Soc. 44, 252 (1967).

Acknowledgments

This work was carried out under the aegis of the Atomic Energy Commission, and with the aid of a Graduate Fellowship from the National Science Foundation to one of us (JBT). The latter would also like to thank University of Canterbury colleagues Leon Phillips and Alan Metcalfe for a number of helpful discussions concerning I_2 adsorption.

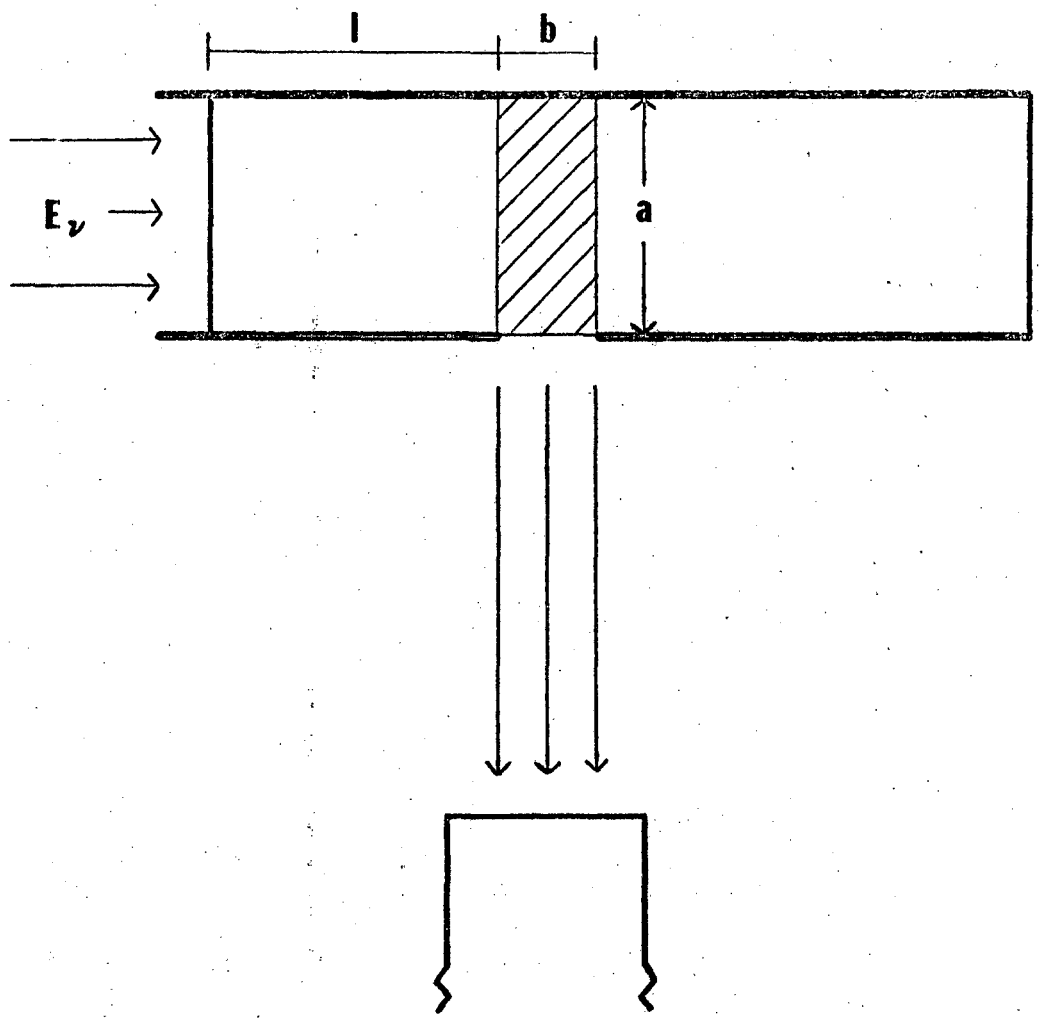

XBL 6910-5809

Figure 1. Schematic of a fluorescence cell.

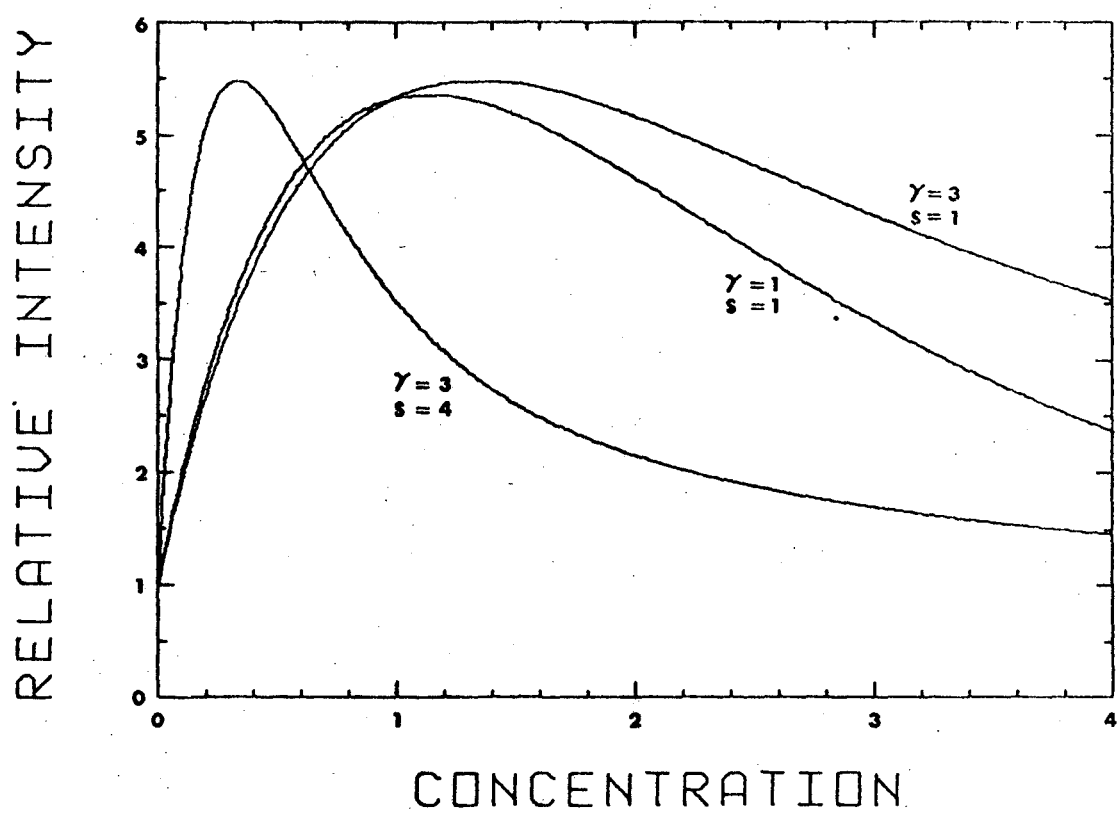

XBL 6910-5810

Figure 2. Fluorescence function plots. γ is the relative linewidth parameter for the Doppler-broadenced emission and absorption lines. s is the relative absorption strength, and concentrations are in arbitrary units such that $k_0 \ell = s\,N$. Intensities are scaled to a 5/1 fluorescence-to-background ratio.

(a) $P(I_2)$ = 8.5 mtorr
1 msec/div.

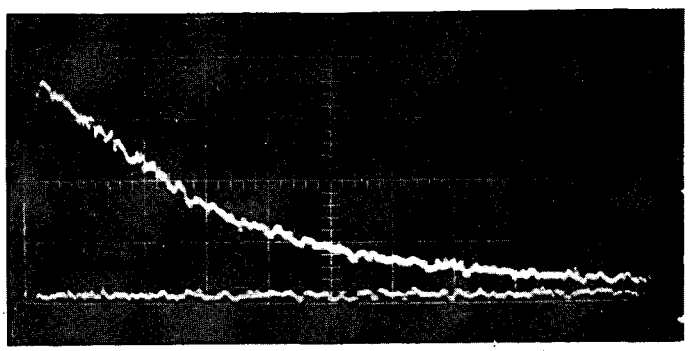

(b) $P(I_2)$ = 56 mtorr
2 msec/div.

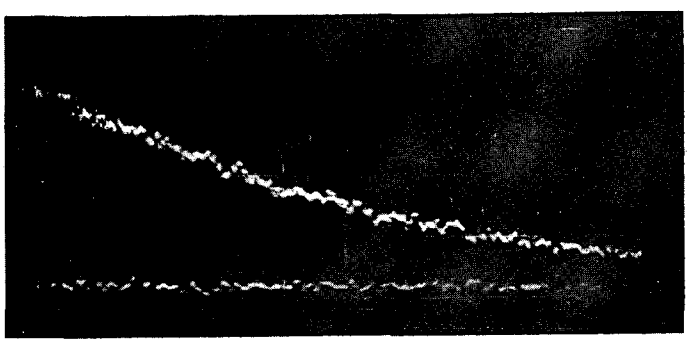

(c) $P(I_2)$ = 156 mtorr
2 msec/div.

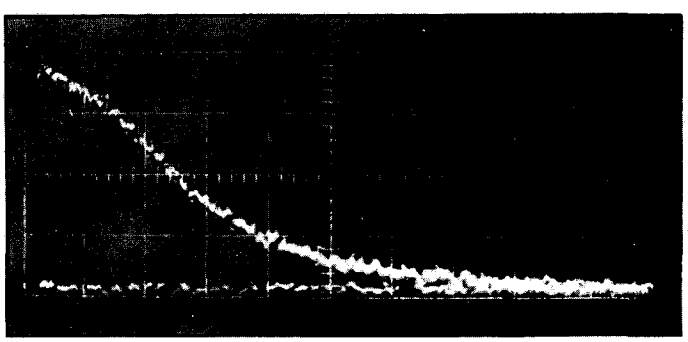

(d) $P(I_2)$ = 129 mtorr
5 msec/div.

XBB6910-6803

Figure 3. Oscilloscope tracings of fluorescence signals from iodine atoms produced with a mild flash discharge.

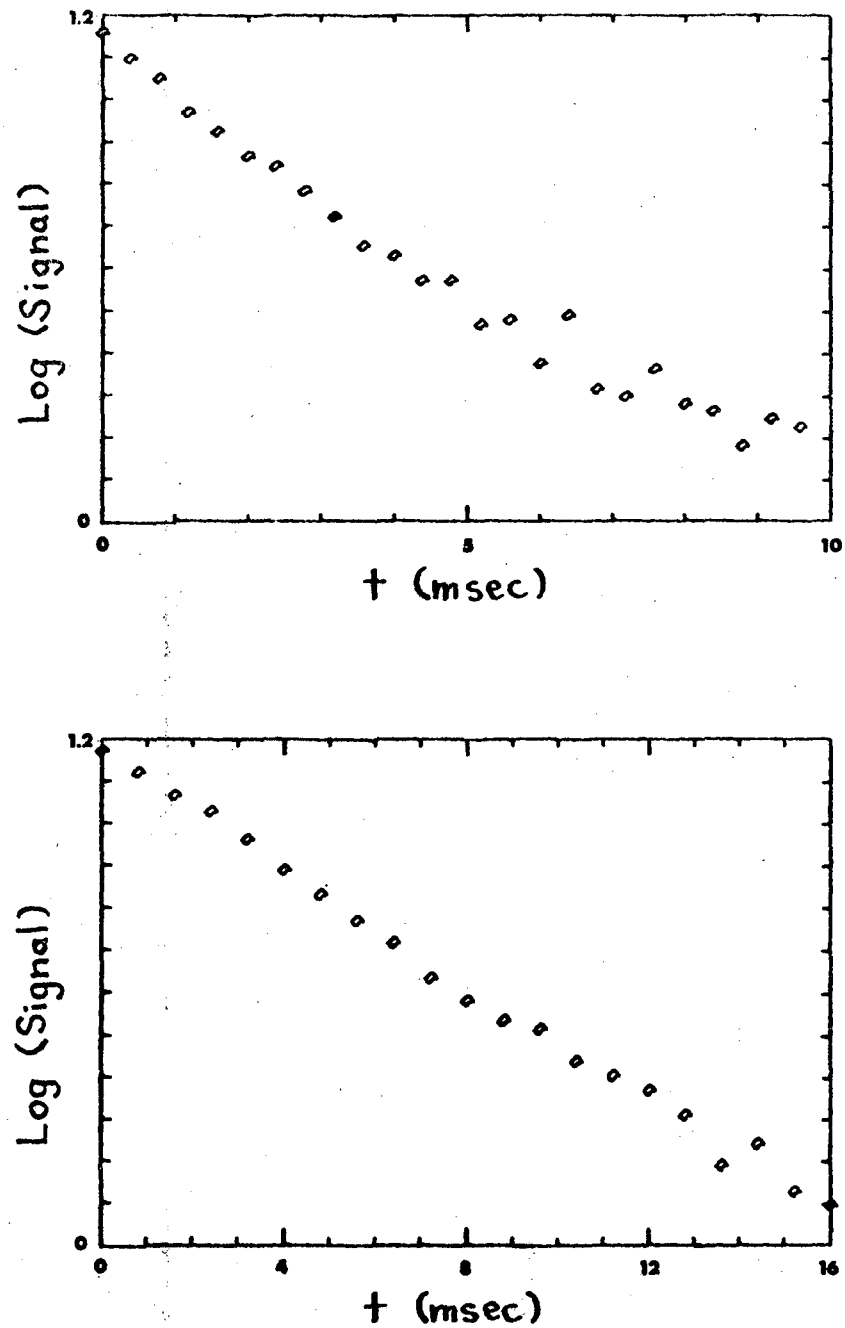

XBL 6910-5813

Figure 4. Logarithmic plots of data from tracings in Fig. 3. Upper plot is for curve (a), $P(I_2)$ = 8.5 mtorr. Lower plot is for curve (b), $P(I_2)$ = 56 mtorr. (Only half the recorded data points are included in these graphs.)

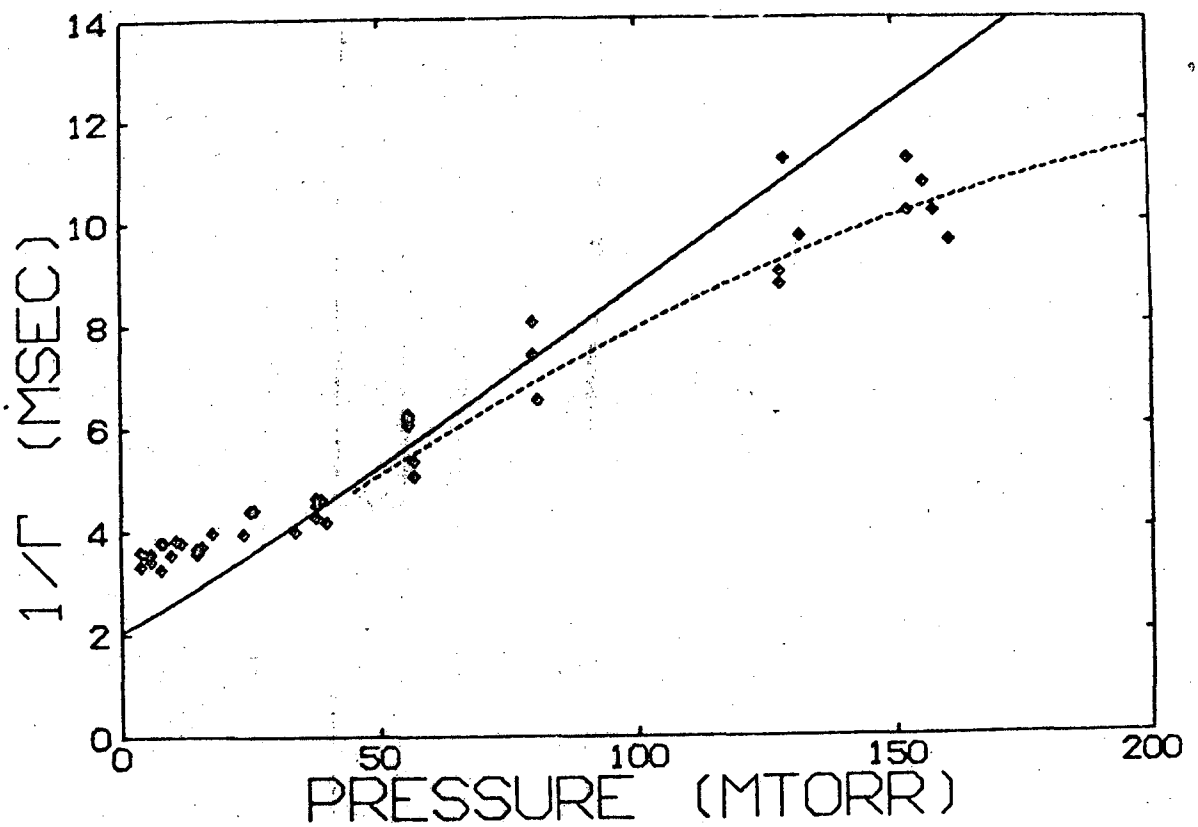

XBL 709-6518

Figure 5. Iodine atom removal rate as a function of I_2 pressure. The solid curve was calculated using $\varepsilon = 0.076$, $D = 7.8$ torr cm^2/sec; the dashed curve includes a homogeneous contribution of the form $\Gamma' = 120\ sec^{-1}\ torr^{-1} \times P_{I_2}$.

LEGAL NOTICE

This report was prepared as an account of Government sponsored work. Neither the United States, nor the Commission, nor any person acting on behalf of the Commission:

A. Makes any warranty or representation, expressed or implied, with respect to the accuracy, completeness, or usefulness of the information contained in this report, or that the use of any information, apparatus, method, or process disclosed in this report may not infringe privately owned rights; or

B. Assumes any liabilities with respect to the use of, or for damages resulting from the use of any information, apparatus, method, or process disclosed in this report.

As used in the above, "person acting on behalf of the Commission" includes any employee or contractor of the Commission, or employee of such contractor, to the extent that such employee or contractor of the Commission, or employee of such contractor prepares, disseminates, or provides access to, any information pursuant to his employment or contract with the Commission, or his employment with such contractor.

TECHNICAL INFORMATION DIVISION
LAWRENCE RADIATION LABORATORY
UNIVERSITY OF CALIFORNIA
BERKELEY, CALIFORNIA 94720